

# Quantum lattice solitons in ultracold bosons near the Feshbach resonance

K V Krutitsky<sup>1</sup> and D V Skryabin<sup>2</sup>

<sup>1</sup> Fachbereich Physik der Universität Duisburg-Essen, Campus Essen,  
Universitätsstr. 5, 45117 Essen, Germany

<sup>2</sup> Department of Physics, University of Bath, Bath, BA2 7AY, UK

E-mail: kostya@theo-phys.uni-essen.de

**Abstract.** Quantum lattice solitons in a system of two ultracold bosons near Feshbach resonance are investigated. It is shown that their binding energy, effective mass, and spatial width, can be manipulated varying the detuning from the Feshbach resonance. In the case of attractive atomic interactions, the molecule creation stabilizes the solitons. In the case of repulsive interactions, the molecule creation leads to the possibility of existence of bright solitons in some interval of detunings. Due to quantum fluctuations the distance between the atoms is a random quantity with the standard deviation larger than the mean value.

## 1. Introduction

Many-body phenomena in ultracold quantum gases is a subject of extensive ongoing research. Interaction between atoms plays a crucial role in many situations and is responsible for the most striking experimental observations of solitons in Bose-Einstein condensates trapped by harmonic [1] and periodic [2] potentials. The typical number of atoms in such solitons varies from several hundreds to tens of thousands. Therefore these structures can be well described by the mean-field Gross-Pitaevsky equation. However, the mean-field theory does never provide an exact description of interacting quantum systems (e.g., due to unavoidable depletion) and it becomes interesting to investigate quantum effects in the soliton propagation [3]. If the atoms are loaded into the optical lattice, the interaction effects become more important and in the limit of the small number of atoms an exact quantum analysis of the solitons [4, 5] reveals strong deviations from the results provided by the Gross-Pitaevsky equation with lattice potential [6] or its discrete version [4, 7].

The use of Feshbach resonances to control interaction between ultracold atoms in optical potentials is a widely spread technique allowing transformation of atoms into molecules and changing magnitude and sign of the effective scattering length of the atoms (see, e.g., [8, 9]). Coherent solitons in condensed atomic-molecular mixtures without optical lattice were studied in several papers, see, e.g., [10, 11]. The mathematical model previously used for the coupled atomic-molecular condensates is equivalent to the model describing parametric interaction of photons in quadratically nonlinear crystals [12]. It was demonstrated in the mean-field limit that the resonant atomic-molecular interaction serves as a mechanism responsible for supporting bright solitons in the case of repulsive bosons and for preventing collapse in the case of attractive bosons [11, 12]. The quantum atomic-molecular solitons in the system without periodic potential were also studied [10, 13]. Optical parametric solitons in the system of coupled waveguides, playing the role of a periodic potential for photons, were recently observed experimentally [14]. Atomic-molecular solitons in a deep optical lattice have been theoretically considered in the mean-field approximation [15], which is mathematically equivalent to the system studied in [14].

In this work, we demonstrate existence and study properties of the quantum atomic-molecular solitons in an optical lattice near Feshbach resonance. Under the quantum lattice soliton we understand the quantum state of the system of interacting particles with the localized eigenfunction and the discrete energy level belonging to a spectral interval forbidden for the spatially extended periodic states [4]. Note that the discrete energy levels belonging to the intervals forbidden for the linear waves are also a generic feature of the classical lattice solitons. Advances in manipulation of ultracold atomic systems with small number of particles per lattice site [16] as well as in cooling and trapping of single atoms [17] allow one to hope that quantum lattice solitons will soon become relevant for experimental research.

## 2. Hamiltonian

We consider two atoms of mass  $m$  in an optical lattice created by a far-detuned standing laser wave. If the laser wavelength is  $\lambda_L = 2\pi/k_L$ , then the lattice constant  $d = \lambda_L/2$ . It is convenient to represent the amplitude of the periodic potential in the form  $\hbar\omega_R s$ , where  $\omega_R = \hbar k_L^2/(2m)$  is the recoil frequency and  $s$  is a dimensionless parameter. In the case of a deep optical lattice every lattice site can be described by a harmonic potential with the frequency  $\omega = 2\omega_R\sqrt{s}$  and the lowest-band atomic Wannier function is well approximated by a Gaussian with the characteristic length  $l_a = \sqrt{\hbar/m\omega}$ . The atoms in the lattice are subject to the magnetic field  $B$ , with  $B = B_0$  corresponding to the Feshbach resonance of the width  $\Delta B$ .

There are several processes which are to be taken into account in such a system: atomic interaction, molecule production and atomic and molecular hopping. Taking into account only the hopping between the nearest lattice sites as well as on-site atomic interactions and in the lowest-band approximation the Hamiltonian of the system is given by [18, 19]

$$H = -t_a \sum_{\langle i,j \rangle} a_i^\dagger a_j - t_m \sum_{\langle i,j \rangle} b_i^\dagger b_j + \left( \delta - \frac{3}{2}\hbar\omega \right) \sum_i b_i^\dagger b_i + \frac{U_{bg}}{2} \sum_i a_i^\dagger a_i^\dagger a_i a_i + \tilde{g} \sum_i \left( b_i^\dagger a_i a_i + a_i^\dagger a_i^\dagger b_i \right), \quad (1)$$

where  $a_i^\dagger$  ( $b_i^\dagger$ ) and  $a_i$  ( $b_i$ ) are creation and annihilation operators of a single atom (molecule) at a lattice site  $i$ ,  $\delta = \Delta\mu(B - B_0)$  is a detuning from the Feshbach resonance. Here,  $\Delta\mu$  is the difference in magnetic moments of the two atoms and a molecule. The atom-molecule conversion is determined by  $\tilde{g} = \hbar\sqrt{2\pi a_{bg}\Delta B\Delta\mu/m}/(2\pi l_a^2)^{3/4}$  and the background on-site atomic interaction parameter is  $U_{bg} = \sqrt{2/\pi}\hbar\omega(a_{bg}/l_a)$  with  $a_{bg}$  being the background scattering length. In the Gaussian approximation, the atomic and molecular tunneling matrix elements are given by  $t_{a,m} = \frac{\hbar\omega}{2} \left[ 1 - \left( \frac{2}{\pi} \right)^2 \right] \left( \frac{\lambda_L}{4l_{a,m}} \right)^2 e^{-(\lambda_L/4l_{a,m})^2}$ . Since  $l_m = l_a/\sqrt{2}$ , the molecular tunneling rate is much smaller than the atomic one.

## 3. Solution of the on-site problem

The on-site problem for the Hamiltonian (1) can be easily solved analytically. In the case when the atoms are on the same lattice site there are two eigenmodes which are superpositions of the two-atom and molecular states with the energies

$$E_{\pm} = \frac{\delta' + U_{bg}}{2} \pm \sqrt{\left( \frac{\delta' - U_{bg}}{2} \right)^2 + 2\tilde{g}^2}, \quad (2)$$

and the probability to find a molecule

$$p_{m\pm} = \frac{1}{2} \left[ 1 \pm \frac{\delta' - U_{bg}}{\sqrt{(\delta' - U_{bg})^2 + 8\tilde{g}^2}} \right], \quad (3)$$

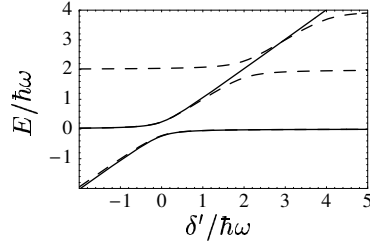


**Figure 1.** Eigenenergies in the case of two atoms on the same lattice site. Solid lines show the results given by Eq. (2) which correspond to the lowest-band approximation. The results for the infinite number of bands [Eq. (4)] are shown by dashed lines.  $U_{\text{bg}} = 0$ ,  $2\sqrt{\pi}\tilde{g}^2/(\hbar\omega)^2 = 0.1$ .

where  $\delta' = \delta - \frac{3}{2}\hbar\omega$  is an effective detuning.

The two-atoms on-site problem was exactly solved in Ref. [18] for the infinite number of bands neglecting the atom-atom interaction. The eigenenergies  $E$  are shown to be determined by the equation

$$E - \delta' = \frac{2\sqrt{\pi}\tilde{g}^2}{\hbar\omega} \frac{\Gamma(-E/2\hbar\omega)}{\Gamma(-E/2\hbar\omega - 1/2)}. \quad (4)$$

The eigenenergies given by Eq. (2) for  $U_{\text{bg}} = 0$  and Eq. (4) are plotted in Fig. 1. As we see, our lower-branch solution  $E_-$  in Eq. (2) is in excellent agreement with the corresponding branch of Eq. (4) for arbitrary  $\delta$ . The upper-branch solution  $E_+$  fails to reproduce the second branch of Eq. (4) if  $\delta$  is far above the Feshbach resonance where the contribution of the second band becomes significant, remaining however in a very good agreement near the resonance and below it. This implies that the lowest-band approximation is valid if the effective detuning  $\delta'$  is less than the gap between the two lowest Bloch bands, which is the quantity of the order of  $\hbar\omega$ , and/or if we are interested in the eigenmodes of the Hamiltonian (1) with the energies less than the energy of the second Bloch band. The latter is always the case in the present work. In addition, the parameters  $U_{\text{bg}}$  and  $\tilde{g}$  must be much smaller than the bands separation which is also fulfilled.

#### 4. Eigenmodes of the complete Hamiltonian and the soliton band

We consider a one-dimensional model with  $L$  lattice sites and assume that  $L$  is odd $\ddagger$ . Under periodic boundary conditions the eigenstates of the Hamiltonian (1) are

$$\begin{aligned} |\psi_k\rangle = & c_k^{\text{m}} \sum_{j=1}^L \left(\hat{T}/\tau_k\right)^{j-1} |1_{\text{m}}0 \dots 0\rangle + c_{0k}^{\text{a}} \sum_{j=1}^L \left(\hat{T}/\tau_k\right)^{j-1} |20 \dots 0\rangle \\ & + c_{1k}^{\text{a}} \sum_{j=1}^L \left(\hat{T}/\tau_k\right)^{j-1} |110 \dots 0\rangle + \dots \end{aligned}$$

$\ddagger$  In the case of even  $L$  there will be only unessential modifications in the equations.

$$+ c_{(L-1)/2,k}^a \sum_{j=1}^L \left( \hat{T}/\tau_k \right)^{j-1} |10 \dots 010 \dots 0\rangle, \quad (5)$$

where  $|1_m 0 \dots 0\rangle$  is a state with one molecule on the first lattice site and all the other sites being unoccupied,  $|n_1 \dots n_L\rangle$  is a state with  $n_i$  atoms on site  $i$ ,  $i = 1, \dots, L$ .  $\hat{T}$  is the translation operator which has the eigenvalues  $\tau_k = \exp(i\pi k/k_L)$  with the wave number  $k = k_L 2\nu/L$ ,  $\nu = 0, \pm 1, \dots, \pm(L-1)/2$  [4]. The eigenvalue problem for the Hamiltonian (1) can be written down in the matrix form

$$\begin{pmatrix} \epsilon_k^m & A^T \\ A & Q_k \end{pmatrix} \begin{pmatrix} c_k^m \\ \mathbf{c}_k^a \end{pmatrix} = E_k \begin{pmatrix} c_k^m \\ \mathbf{c}_k^a \end{pmatrix}, \quad (6)$$

where  $\epsilon_k^m = \delta' - 2t_m \cos(\pi k/k_L)$ . The vector  $A$  has a length  $(L+1)/2$  and its nonvanishing element is  $A_1 = \sqrt{2}\tilde{g}$ . The nonvanishing elements of the tridiagonal  $(L+1)/2 \times (L+1)/2$  matrix  $Q_k$  are given by [4]

$$\begin{aligned} Q_{11} &= U_{bg}, \quad Q_{21} = Q_{12}^* = -t_a \sqrt{2}(1 + \tau_k), \\ Q_{i+1,i} &= Q_{i,i+1}^* = -t_a(1 + \tau_k), \quad i = 2, \dots, (L-1)/2, \\ Q_{(L+1)/2,(L+1)/2} &= -t_a \left[ \tau_k^{(L+1)/2} + \tau_k^{(L-1)/2} \right]. \end{aligned} \quad (7)$$

The eigenvectors in Eq. (6) consist of two parts  $c_k^m$ ,  $\mathbf{c}_k^a = \text{col}[c_{0k}^a, \dots, c_{(L-1)/2,k}^a]$ , and satisfy the normalization condition

$$|c_k^m|^2 + \sum_{i=0}^{(L-1)/2} |c_{ik}^a|^2 = 1. \quad (8)$$

In the absence of the molecular mode, the eigenvalue problem (6) reduces to that one solved in Ref. [4], where it was shown that in the case of attractive interaction the energy spectrum consists always of (quasi)continuum band and a discrete level below the (quasi)continuum which corresponds to the bright soliton. Its characteristic feature is that  $|c_{0k}^a|^2 \gg |c_{ik}^a|^2$ ,  $i = 1, \dots, (L-1)/2$ , i.e., the probability of finding two atoms on the same lattice site is much higher than all the other ones. This localization corresponds to the soliton solution of the discrete nonlinear Schrödinger equation and, therefore, the discrete level can be called a "soliton band" [4]. Our aim is to investigate the influence of the molecular mode on the soliton band.

After the eigenvalue problem (6) is solved, one can calculate the soliton binding energy  $E_b$  which is defined as the difference of the energy at the bottom of the (quasi)continuum and the soliton level at  $\nu = 0$  which corresponds to  $k = k_0 = 0$ . The effective mass  $m^*$  can be worked out using a quadratic approximation for the eigenenergy at some small value of  $\nu$  (e.g.,  $\nu = 1$ )  $E_{k_1} = E_{k_0} + \hbar^2 k_1^2 / (2m^*)$ , which leads to

$$m^* = 2\hbar^2 k_L^2 / [(E_{k_1} - E_{k_0}) L^2]. \quad (9)$$

According to Eq. (5) the distance between the atoms  $w_k$  is a random variable which takes the values  $w_{ki} = 0, 1, \dots, (L-1)/2$ , with the probabilities  $|c_{ik}^a|^2 / (1 - |c_k^m|^2)$ . Thus, it is

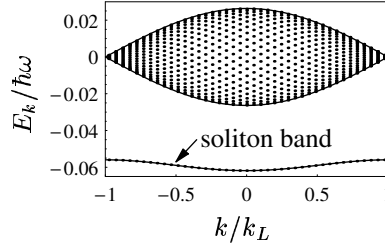


**Figure 2.** Energy eigenvalues of the Hamiltonian (1). The parameters are  $s = 5$ ,  $2\sqrt{\pi}\tilde{g}^2/(\hbar\omega)^2 = 0.1$ ,  $\delta'/\hbar\omega = 3$ ,  $a_{\text{bg}}/\lambda_L = -0.005$ . Dots are the results of numerical solution of Eq. (6) for  $L = 41$  and the solid lines correspond to the limit  $L \rightarrow \infty$ . The spectrum is truncated from above in order to be consistent with the lowest-band approximation.

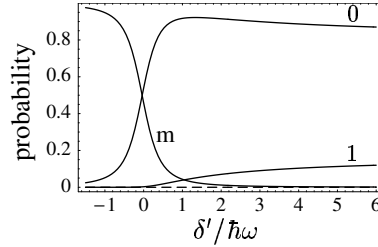


**Figure 3.** Probabilities of molecular and atomic states corresponding to the soliton band:  $|c_0^{\text{m}}|^2$  (m),  $|c_{i0}^{\text{a}}|^2$  (i),  $i = 0, 1, 2$  [ $|c_{20}^{\text{a}}|^2$  is shown by the dashed line]. The parameters are the same as in Fig. 2.

necessary to calculate not only the mean interatomic distance  $\langle w_k \rangle$  but also its standard deviation

$$\sigma_{wk} = \sqrt{\langle w_k^2 \rangle - \langle w_k \rangle^2}, \quad \langle w_k^l \rangle = \sum_{i=0}^{(L-1)/2} \frac{i^l |c_{ik}^{\text{a}}|^2}{1 - |c_k^{\text{m}}|^2}, \quad (10)$$

and the soliton width can be defined as  $\sqrt{\langle w_k^2 \rangle}$ .

We have solved the eigenvalue problem (6) numerically for finite values of  $L$  and analytically in the limit of infinite lattice. The results are presented below. We consider the cases of attractive and repulsive atomic interactions and concentrate on the properties of the lower-energy modes.

#### 4.1. Attractive atomic interaction

We consider first bosons with attractive interactions ( $U_{\text{bg}} < 0$ ). If  $\delta'$  is negative and its absolute value is very large, the coupling between the molecular mode and the atomic mode is negligible and we have two discrete levels below the (quasi)continuum. The lower one corresponds to the pure molecule and another one to the atomic bright soliton. If  $\delta'$  increases, i.e., we come closer to the Feshbach resonance, both discrete levels approach the (quasi)continuum. At some critical value of  $\delta' = \delta'_-$  the upper level merges with the (quasi)continuum. In the numerical calculations it is not quite clear how to determine  $\delta'_-$  exactly because there are several possibilities to define it. Analytical analysis in

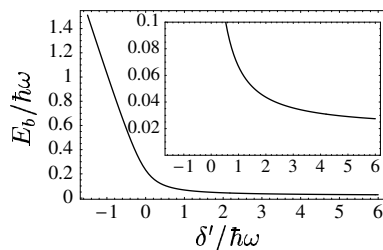


**Figure 4.** Soliton binding energy. The parameters are the same as in Fig. 2 and  $k = 0$ .

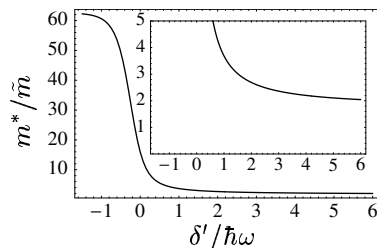


**Figure 5.** The ratio of the soliton effective mass  $m^*$  to the effective mass  $\tilde{m}$  at the bottom of (quasi)continuum band. The parameters are the same as in Fig. 2.

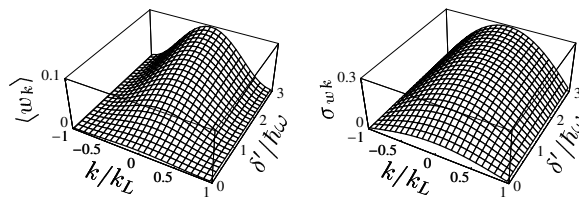


**Figure 6.** Mean interatomic distance  $\langle w_k \rangle$  (left panel) and its standard deviation  $\sigma_{wk}$  (right panel). The parameters are the same as in Fig. 2.

the case of the infinite lattice shows that the mergence occurs if at least one of the inequalities

$$|c_{1k}^a| > |c_{ik}^a|, i = 2, 3, \dots, \quad (11)$$

is violated. We adopt this as a definition of  $\delta'_-$  and by doing numerical diagonalization for  $k = 0$  and for the values of parameters in the caption of Fig. 2 we obtain  $\delta'_- = -1.531 \hbar\omega$ . In order to have inequalities (11) again fulfilled, one has to increase  $\delta'$  up to  $\delta'_+$ . Using the same values of the parameters we get  $\delta'_+ = -1.490 \hbar\omega$ . If  $\delta' > \delta'_+$ , a discrete level appears above the (quasi)continuum, while the lower one which becomes a linear combination of atomic and molecular states remains below (see Fig. 2). If we increase  $\delta'$  further and go far away from the Feshbach resonance ( $\delta' \gg \hbar\omega$ ), the contribution of the molecular mode into the lowest-energy eigenstate becomes negligible (Fig.3) and we have a pure atomic bright soliton below the (quasi)continuum [4]. The upper discrete level is located very far above the (quasi)continuum and cannot be interpreted within

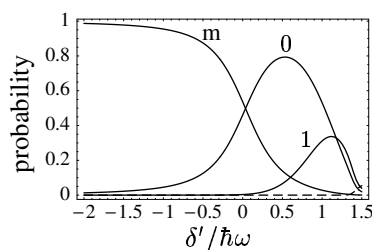


**Figure 7.** Probabilities of molecular and atomic states corresponding to the soliton band:  $|c_0^m|^2$  (m),  $|c_{i0}^a|^2$  ( $i$ ),  $i = 0, 1, 2$  [ $|c_{20}^a|^2$  is shown by the dashed line].  $a_{bg}/\lambda_L = 0.005$  and the other parameters are the same as in Fig. 2.

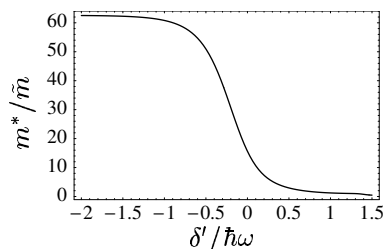


**Figure 8.** The ratio of the soliton effective mass  $m^*$  to the effective mass  $\tilde{m}$  at the bottom of (quasi)continuum band. The parameters are the same as in Fig. 7.

the lowest-band approximation.

The soliton binding energy  $E_b$  is shown in Fig. 4. Due to the large contribution of the molecular mode near the resonance the binding energy is larger than its asymptotic value at  $\delta' \rightarrow \infty$ . The effective mass  $m^*$  is also larger at smaller values of  $\delta'$  (see Fig. 5) because due to the fact that  $t_m \ll t_a$  the effective mass of the molecule is much larger than the atomic effective mass. The corresponding contributions of the molecular and atomic states into the soliton band are shown in Fig. 3.

The mean interatomic distance  $\langle w_k \rangle$  as well as its standard deviation  $\sigma_{wk}$  are shown in Fig. 6. The interatomic distance is well below the lattice constant  $d$  and the maximal localization is achieved at the edges of the Brillouin zone. However, quantum fluctuations are very strong and  $\sigma_{wk} > \langle w_k \rangle$ .

#### 4.2. Repulsive atomic interaction

In the case of repulsive atomic interaction ( $U_{bg} > 0$ ), the situation is quite different. There can be only one discrete level below the (quasi)continuum which is occupied by the molecule as long as  $\delta'$  is negative and its absolute value remains very large. Above the (quasi)continuum, there is another discrete level corresponding to the atomic bright soliton. If we increase  $\delta'$  the lower discrete level approaches the (quasi)continuum and the probabilities of the atomic states become larger meaning that the system enters the bright soliton regime supported by the molecule creation (see Fig. 7). Inequalities (11) are satisfied in this regime. If we increase  $\delta'$  further and reach the value  $\delta'_-$ , the probability of the molecular state becomes very small. Inequalities (11) are violated and



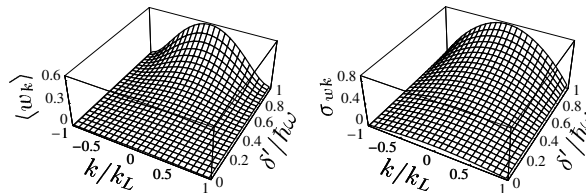


**Figure 9.** Mean interatomic distance  $\langle w_k \rangle$  (left panel) and its standard deviation  $\sigma_{wk}$  (right panel). The parameters are the same as in Fig. 7.

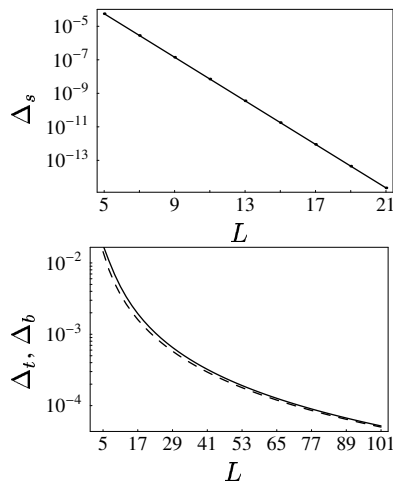


**Figure 10.** Deviations of the eigenvalues of Eq.(6) for finite  $L$  from that obtained in the limit  $L \rightarrow \infty$ .  $\Delta_t$  is shown by the dashed line. The parameters are the same as in Fig. 2.

the discrete level merges with the (quasi)continuum, i.e., the bright soliton is destroyed. The probability  $|c_k^m|^2$  can be also interpreted as a relative population of the molecular component. It is a decreasing function of  $\delta'$  like in the case of classical atomic-molecular solitons [15].

If the detuning is further increased up to  $\delta'_+$ , the soliton band appears above the (quasi)continuum. For the values of parameters used in our numerical estimations,  $\delta'_- = 1.479 \hbar\omega$  and  $\delta'_+ = 1.521 \hbar\omega$ .

The soliton binding energy  $E_b$  is again a decreasing function of  $\delta'$  which vanishes at  $\delta' = \delta'_-$ . The effective mass  $m^*$  equals to the effective mass of the molecule for large negative  $\delta'$  and reaches the value  $\tilde{m}$  at  $\delta' = \delta'_-$  (Fig. 8). If we come closer to  $\delta'_-$  the solitons become less localized especially at  $k = 0$  and the interatomic-distance fluctuations increase (Fig. 9). According to our definition of the soliton width, its behavior is similar to that of  $\langle w_k \rangle$  and  $\sigma_{wk}$  shown in Fig. 9.

### 4.3. The limit $L \rightarrow \infty$

In the limit  $L \rightarrow \infty$ , the wave number  $k$  becomes a continuous variable. The energies of the continuum band are enclosed in the interval  $|E_k| \leq q_k$ , where  $q_k = 4t_a \cos\left(\frac{\pi k}{2k_L}\right)$ , and the coefficients  $c_{0k}^a$ ,  $c_k^m$ , in Eq. (6) become negligibly small. Outside of the continuum band, the solutions have the form  $c_{jk}^a = a_k b_k^j \exp\left(i\frac{\pi k}{2k_L}j\right)$ ,  $j = 1, 2, \dots, \infty$ . Substituting this ansatz into Eq. (6) we obtain the equation for the eigenenergy  $\mathcal{E}_k = \lim_{L \rightarrow \infty} E_k$

$$\mathcal{E}_k^2 = (U_{\text{bg}} + U_k)^2 + q_k^2, \quad U_k = 2\tilde{g}^2 / (\mathcal{E}_k - \epsilon_k^m). \quad (12)$$

Note that the quantity  $U_{\text{bg}} + U_k$  plays a role of the effective atomic interaction. The values of  $a_k$  and  $b_k$  corresponding to a certain  $\mathcal{E}_k$  are given by  $a_k = \sqrt{2}c_{0k}^a$ ,  $b_k = (U_{\text{bg}} + U_k - \mathcal{E}_k)/q_k$ , and the expressions for the probabilities of the state with two atoms on the same lattice site and the molecular state take the form

$$\begin{aligned} |c_{0k}^a|^2 &= (1 - b_k^2) / [1 + b_k^2 + (1 - b_k^2) S_k], \\ |c_k^m|^2 &= 2\tilde{g}^2 |c_{0k}^a|^2 / (\mathcal{E}_k - \epsilon_k^m)^2, \end{aligned} \quad (13)$$

where  $S_k = 2\tilde{g}^2 / (\mathcal{E}_k - \epsilon_k^m)^2$ .

Eq. (12) can be multiplied by  $(\mathcal{E}_k - \epsilon_k^m)^2$  and treated as quartic equation for  $\mathcal{E}_k$  which contains always four roots. However, depending on the values of the parameters only one or two roots are real and provide normalized eigenstates implying that the others are unphysical and should be rejected. The normalization condition (8) requires  $a_k^2/2 < 1$  as well as  $|b_k| < 1$ . One can easily show that in the special case  $t_a = t_m = 0$  the physical solutions of Eq. (12) are given by (2).

We substitute  $\mathcal{E}_{k\pm} = \pm q_k$  corresponding to the edges of the continuum band into Eq.(12) and get

$$U_{\text{bg}} + U_{k\pm} = 0, \quad (14)$$

which leads to the identity  $|b_k| = 1$  and as a consequence to the violation of inequalities (11). Eq. (14) allows to obtain the boundaries  $\delta'_-$  and  $\delta'_+$  of the interval of  $\delta'$  within which there is only one physical solution:

$$\delta'_{\pm} = \pm q_k + 2t_m \cos(\pi k/k_L) + 2\tilde{g}^2/U_{\text{bg}}. \quad (15)$$

For the values of parameters used in the numerical diagonalization, we find  $\delta'_- = -1.531 \hbar\omega$  and  $\delta'_+ = -1.479 \hbar\omega$  in the case of attractive interaction, and  $\delta'_- = 1.479 \hbar\omega$  and  $\delta'_+ = 1.532 \hbar\omega$  in the case of repulsive interaction. The values of  $\delta'_-$  are in perfect agreement with the results of numerical calculations for  $L = 41$ , while  $\delta'_+$  have small deviations from the corresponding numerical estimations. In the special case  $t_a = t_m = 0$ ,  $\delta'_- = \delta'_+ = \delta'_*$  and Eq. (14) leads to the condition

$$U_{\text{bg}} - 2\tilde{g}^2/\delta'_* = 0. \quad (16)$$

This is equivalent to the requirement that the effective scattering length  $a_{\text{bg}}(1 - \Delta B \Delta\mu/\delta')$ , which appears in the mean-field theory as a result of the adiabatic elimination of the molecular field [8], vanishes. The calculations presented above show

that in the interval of the detunings  $\delta'_- < \delta' < \delta'_+$  the effective atomic interaction is gradually switched from the attractive to the repulsive one.

The probabilities  $|c_{jk}^a|^2$ ,  $j = 1, 2, \dots$ , of the atomic states in Eq.(5) decrease with  $j$  and have the form

$$|c_{ik}^a|^2 = (1 - b_k^2) b_k^{2(i-1)} [1 - |c_{0k}^a|^2 (1 + S_k)] . \quad (17)$$

The soliton effective mass

$$m^* = \hbar^2 \left( \frac{\partial^2 \mathcal{E}_k}{\partial k^2} \Big|_{k=0} \right)^{-1} = \hbar^2 \frac{\mathcal{E}_k + (U_{\text{bg}} + U_k) S_k}{2t_m (U_{\text{bg}} + U_k) S_k - 4t_a^2} \Big|_{k=0} \quad (18)$$

is smaller than that at the bottom of the continuum

$$\tilde{m} = \hbar^2 \left( - \frac{\partial^2 q_k}{\partial k^2} \Big|_{k=0} \right)^{-1} = \frac{\hbar^2 k_L^2}{\pi^2 t_a} . \quad (19)$$

The first two moments of the interatomic-distance distribution can be shown to be

$$\begin{aligned} \langle w_k \rangle &= 2 |c_{0k}^a|^2 b_k^2 / \left[ (1 - b_k^2)^2 (1 - |c_k^m|^2) \right] , \\ \langle w_k^2 \rangle &= 2 |c_{0k}^a|^2 b_k^2 (1 + b_k^2) / \left[ (1 - b_k^2)^3 (1 - |c_k^m|^2) \right] . \end{aligned} \quad (20)$$

In order to demonstrate the convergence to the limit  $L \rightarrow \infty$ , we have plotted in Fig. 10 the quantities  $\Delta_s = \sup_k |E_k^{(s)} - \mathcal{E}_k| / \hbar\omega$  as well as  $\Delta_t = \sup_k |E_k^{(t)} - q_k| / \hbar\omega$  and  $\Delta_b = \sup_k |E_k^{(b)} + q_k| / \hbar\omega$  for different  $L$ , where  $E_k^{(s)}$ ,  $E_k^{(t)}$ , and  $E_k^{(b)}$  are the eigenenergies of Eq.(6) corresponding to the soliton band, the top and the bottom of the quasi-continuum band, respectively.  $\Delta_s$  decreases exponentially with the increase of  $L$  and it is very small even for low values of  $L$ . The convergence for the boundaries of the continuum band is slower, but the limit  $L \rightarrow \infty$  describes quite well the results of the numerical diagonalization already for a few tens of the lattice sites. In addition, we have compared the results of the calculations obtained on the basis of numerical solution of the eigenvalue problem (6) for  $L = 41$  which are presented in Figs. 2-9 with that worked out in the limit  $L \rightarrow \infty$  and did not find any noticeable discrepancies. This is consistent with the exponential decrease of  $\Delta_s(L)$ .

In the absence of the magnetic field, the molecule creation is impossible and one has to put  $\tilde{g} = 0$ ,  $\delta' = 0$ ,  $t_m = 0$ , in all the equations. In this special case, the normalizable solution of Eq. (12) is given by  $\mathcal{E}_k^{(0)} = \text{sign}(U_{\text{bg}}) \sqrt{U_{\text{bg}}^2 + q_k^2}$ , which leads to the following expression for the effective mass  $m^{*(0)} = -\hbar^2 \text{sign}(U_{\text{bg}}) \sqrt{U_{\text{bg}}^2 + 16t_a^2} / (4t_a^2)$ . These are exactly the results presented in Ref. [4]. The soliton band exists again for repulsive as well as attractive atomic interaction, but in the case of repulsive interaction it appears to be a highly excited mode with the energy above the continuum band.

## 5. Conclusion

Summarizing, we have investigated quantum lattice solitons in a system of two ultracold bosons near the Feshbach resonance. Binding energy, effective mass, and spatial width of the solitons, can be manipulated varying the detuning from the Feshbach resonance.

In the case of attractive atomic interactions, the molecule creation stabilizes the solitons increasing their effective mass as well as the binding energy and decreasing the width. In the case of repulsive interactions, the molecule creation leads to the possibility of existence of bright solitons in some interval of detunings analogous to the corresponding classical system. The presence of quantum fluctuations leads to the fact that the interatomic distance is a random quantity. Its standard deviation is even larger than the mean value.

The classical limit of the problem studied in the present work was considered in [15]. Our results for the relative populations of the atomic and molecular components are in agreement with the corresponding classical results. In order to understand the transition from quantum to classical solitons it is necessary to perform analogous calculations for higher number of atoms. This can be done employing the same method as in the present study. However, one has to keep in mind that the dimension of the Hilbert space increases rapidly with the increase of the particle number and the number of lattice sites.

## Acknowledgments

This work was partly supported by the INTAS (Project No. 01-855) and SFB/TR 12. K.V.K. would like to thank the University of Bath for kind hospitality.

## References

- [1] Burger S, Bongs K, Dettmer S, Ertmer W, Sengstock K, Sanpera A, Shlyapnikov G V and Lewenstein M 1999 *Phys. Rev. Lett.* **83** 5198  
Denschlag J et al 2000 *Science* **287** 97  
Strecker K E, Partridge G B, Truscott A G and Hulet R G 2002 *Nature* **417** 150  
Khaykovich L, Schreck F, Ferrari G, Bourdel T, Cubizolles J, Carr L D, Castin Y and Salomon C 2002 *Science* **296** 1290
- [2] Eiermann B, Anker Th, Albiez M, Taglieber M, Treutlein P, Marzlin K P and Oberthaler M K 2004 *Phys. Rev. Lett.* **92**, 230401
- [3] Dziarmaga J and Sacha K 2002 *Phys. Rev. A* **66** 043620  
Law C K, Leung P T and Chu M C 2002 *J. Phys. B: At. Mol. Opt. Phys.* **35** 3583  
Law C K 2003 *Phys. Rev. A* **68** 015602  
Dziarmaga J 2004 *Phys. Rev. A* **70** 063616  
Buljan H, Segev M and Vardi A 2005 *Phys. Rev. Lett.* **95** 180401
- [4] Scott A C 1999 *Nonlinear science* (Oxford University Press) Ch. 8 and references therein
- [5] Dornig J, Eilbeck J C, Salerno M and Scott A C 2004 *Phys. Rev. Lett.* **93** 025504  
Eilbeck J C and Palmero F 2004 *Phys. Lett. A* **331** 201
- [6] Yulin A V, Skryabin D V and Russell P St J 2003 *Phys. Rev. Lett.* **91** 260402
- [7] Trombettoni A, Smerzi A and Bishop A R 2002 *Phys. Rev. Lett.* **88** 173902
- [8] Moerdijk A J, Verhaar B J and Axelsson A 1995 *Phys. Rev. A* **51** 4852
- [9] Zwierlein M W, Stan C A, Schunck C H, Raupach S M F, Gupta S, Hadzibabic Z and Ketterle W 2003 *Phys. Rev. Lett.* **91** 250401  
Dürr S, Volz Th, Marte A and Rempe G 2004 *Phys. Rev. Lett.* **92** 020406
- [10] Drummond P D, Kheruntsyan K V and He H 1998 *Phys. Rev. Lett.* **81** 3055
- [11] Vaughan T G, Kheruntsyan K V and Drummond P D 2004 *Phys. Rev. A* **70** 063611

- [12] Buryak A V, Trapani P D, Skryabin D V and Trillo S 2002 *Physics Reports* **370** 63 and references therein
- [13] Drummond P D and He H 1997 *Phys. Rev. A* **56** R1107  
Kheruntsyan K V and Drummond P D 1998 *Phys. Rev. A* **58** R2676  
Kheruntsyan K V and Drummond P D 1998 *Phys. Rev. A* **58** 2488  
Kheruntsyan K V and Drummond P D 2000 *Phys. Rev. A* **61** 063816  
Drummond P D and Kheruntsyan K V 2004 *Phys. Rev. A* **70** 033609
- [14] Iwanow R, Schiek R, Stegeman G I, Pertsch T, Lederer F, Min Y and Sohler W 2004 *Phys. Rev. Lett.* **93** 113902
- [15] Abdullaev F Kh and Konotop V V 2003 *Phys. Rev. A* **68** 013605
- [16] Greiner M, Mandel O, Esslinger T, Hänsch Th W and Bloch I 2002 *Nature* **415** 39
- [17] Pinkse P W H, Fischer T, Maunz P and Rempe G 2000 *Nature* **404** 365  
Maunz P, Puppe T, Schuster I, Syassen N, Pinkse P W H and Rempe G 2004 *Nature* **428** 50
- [18] Dickerscheid D B M, Khawaja U Al, van Oosten D and Stoof H T C 2005 *Phys. Rev. A* **71** 043604
- [19] Diener R B and Ho T L 2006 *Phys. Rev. A* **73** 017601  
Dickerscheid D B M, van Oosten D and Stoof H T C 2006 *Phys. Rev. A* **73** 017602